

# Neuropathology of Mowat–Wilson Syndrome

*Pediatric and Developmental Pathology*  
2020, Vol. 23(4) 322–325  
© 2020, Society for Pediatric Pathology  
All rights reserved.  
Article reuse guidelines:  
sagepub.com/journals-permissions  
DOI: 10.1177/1093526620903956  
journals.sagepub.com/home/pdp



Miriam R. Conces<sup>1,2</sup>, Anna Hughes<sup>1</sup>, and Christopher R. Pierson<sup>1,2,3</sup>

## Abstract

Mowat–Wilson syndrome (MWS) is a syndromic form of Hirschsprung disease that is characterized by variable degrees of intellectual disability, characteristic facial dysmorphism, and a diverse set of other congenital malformations due to haploinsufficiency of *ZEB2*. A variety of brain malformations have been described in neuroimaging studies of MWS patients, and the role of *ZEB2* in the brain has been studied in a multitude of genetically engineered mouse models that are now available. However, a paucity of autopsy information limits our ability to correlate data from neuroimaging studies and animal models with actual MWS patient tissues. Here, we report the autopsy neuropathology of a 19-year-old male patient with MWS. Autopsy neuropathology findings correlated well with the reported MWS neuroimaging data and are in keeping with data from genetically engineered MWS mouse models. This autopsy enhances our understanding of *ZEB2* function in human brain development and demonstrates the reliability of MWS murine models.

## Keywords

autopsy, microcephaly, Mowat–Wilson syndrome, neuropathology, *ZEB2*

## Introduction

Mowat–Wilson syndrome (MWS; OMIM 235730) is an autosomal dominant disorder characterized by variable degrees of intellectual disability, facial dysmorphism, callosal agenesis, Hirschsprung disease, and a variety of other malformations including genitourinary and cardiac anomalies. Mowat et al. were the first to describe the syndrome in 6 patients with characteristic facial appearance and Hirschsprung disease<sup>1</sup> and its association with *ZEB2* mutation followed.<sup>2,3</sup> MWS is due to mutations causing haploinsufficiency of *ZEB2*, which encodes Zeb2, a transcriptional regulator.<sup>4</sup> Garavelli et al. delineated the spectrum of brain structural abnormalities in a neuroimaging study of 54 MWS patients which included anomalies of the corpus callosum (79.6%) and hippocampus (77.8%), ventriculomegaly (68.5%), white matter abnormalities (40.7%), and focal signal alterations (22.2%) among others.<sup>5</sup> However, MWS autopsy information is limited<sup>6</sup> so the neuropathological substrate of these imaging findings remains poorly characterized or unknown. Furthermore, a number of genetically engineered mouse models have been generated, but the dearth of human autopsies has limited our ability to correlate them with patient neuropathology. Here, we report the

autopsy neuropathology of a 19-year-old male MWS patient and correlate it with data from neuroimaging studies and murine models in an effort to expand our understanding of *ZEB2* function in human brain development.

## Case Report

The subject was a 19-year-old male diagnosed by clinical criteria with MWS, spastic cerebral palsy, epilepsy, intellectual disability, ventilator-dependent chronic respiratory insufficiency, surgically corrected Hirschsprung disease, scoliosis, and recurrent urinary tract infections. He had been seizure free for months but was admitted

<sup>1</sup>Department of Pathology & Laboratory Medicine, Nationwide Children's Hospital, Columbus, Ohio

<sup>2</sup>Department of Pathology, The Ohio State University, Columbus, Ohio

<sup>3</sup>Division of Anatomy, Department of Biomedical Education & Anatomy, The Ohio State University, Columbus, Ohio

### Corresponding Author:

Christopher R Pierson, Department of Pathology & Laboratory Medicine, Nationwide Children's Hospital, J0359 700 Children's Drive, Columbus, OH 43205, USA.

Email: Christopher.pierson@nationwidechildrens.org

following a seizure. While hospitalized, he continued to seize and developed fever, *Clostridium difficile* toxin-positive watery stool, and urinary tract infection. Acute onset of bloody output from his colostomy site and abdominal distention ensued. He failed to improve and succumbed 9 days after admission. Consent was obtained for a complete autopsy.

### Systemic Autopsy Findings

At autopsy, the crown-heel length was 112 cm and body mass was 41.8 kg, which were both less than the third percentile for age and gender. The face was dysmorphic with a square shape; high forehead; broad and flattened nasal bridge and prominent nasal tip; thick eyebrows; hypertelorism; posteriorly rotated ears with thick, uplifted lobes; central fullness and lateral thinning of the upper lip and mandibular prognathism. There was marked scoliosis. All extremities showed contractures and distal atrophy; the feet showed varus deformities. The lungs were congested and showed abnormal lobation. There were dense peritoneal adhesions and an intact Roux-en-Y anastomosis. The large intestine was dilated due to gas; there was no evidence of gastrointestinal obstruction, perforation, or stenosis. The patient died of complications from acute bronchopneumonia, and autopsy blood cultures isolated *Klebsiella pneumoniae*.

### Neuropathology Findings

The formalin-fixed brain was 1064.1 g (95% confidence limits: 1395.2–1498.0 g; mean: 1446.6 g for age and gender). The cerebrum was small with ill-defined temporal sulcal pattern bilaterally and partially exposed insulae (Figure 1(A)). The cerebellum appeared relatively large compared to the cerebrum (hindbrain: 162 g; Figure 1(B)). The putamen and head of the caudate nucleus seemed generous in size (Figure 1(C)) and appeared unremarkable histologically (Figure 1(D)). Coronal sections revealed unremarkable thalami, callosal agenesis, and cingulate gyri with a complex profile; the hippocampi were small and malrotated (Figure 1(E)). The hilum of the dentate gyrus was wider than expected with reduced numbers of granule cells (Figure 1(F) and (G)). Hippocampal sclerosis was not present. Multiple gray matter heterotopias were noted in cerebral white matter (Figure 1(C), (E), and (H)). The cerebellum and brainstem appeared well developed with focal loss of Purkinje and granule cells in the former (Figure 1(B) and (I)). White matter areas subjacent to the cortex and near the ventricle showed patchy areas of attenuated Luxol fast

blue-periodic acid-Schiff (LFB/PAS) staining and variable attenuation in anti-neurofilament and anti-CNPase immunoreactivity (Figure 1(J)). In areas of white matter with attenuated LFB staining, scattered PAS-positive structures that immunohistochemically labeled with anti-neurofilament antibodies were present and suggestive of possible axonal injury (Figure 1(K)).

### Discussion

We present the neuropathology of a 19-year-old male patient who had many of the characteristic features of MWS, the diagnosis of which was based on clinical criteria as gene testing results were unavailable.<sup>7</sup> During early embryonic development, *Zeb2* is expressed in neural tube and neural crest, and some of the clinical features of MWS can be attributed to crestopathy.<sup>4</sup> Later in development, *Zeb2* is widely expressed in the forebrain and *ZEB2* haploinsufficiency during this developmental window seems to account for most of the central nervous system pathology in MWS patients. Overall, the neuropathologic findings reported here correlate well with the anomalies noted in neuroimaging studies and experimental findings in genetically engineered mouse models.

Autopsy gross findings included callosal agenesis, poorly rotated hippocampi, potentially large basal ganglia, and patchy attenuation of cerebral white matter staining, which aligned with the reported neuroimaging data.<sup>5</sup> Our subject had microcephaly, which occurs in most MWS subjects.<sup>7</sup> However, ventriculomegaly, a common anomaly noted in imaging studies, was not detected at autopsy perhaps due to the presence of callosal agenesis and potentially enlarged basal ganglia. Our case exhibited mild cerebral cortical anomalies with exposed insular cortex and indistinct temporal sulcation. Unfortunately, neuroimaging studies were not available for review, so if this patient had a focal signal alteration as has been described in some MWS subjects, we were unable to perform a direct neuropathologic correlation. A reported MWS autopsy of a 35-week gestation male revealed a short corpus callosum and cerebral white matter edema and gliosis with perivascular mineralizations; however, these white matter changes were not evident in our patient, perhaps due to differences in the ages of the subjects.<sup>6</sup>

Human autopsy data are important because to date most of the information we have about *Zeb2* function in brain development is from genetically engineered mouse models. Mouse and human MWS differ in important respects. Mouse models require the use of conditional *Zeb2* inactivation in order to avoid embryonic lethality,

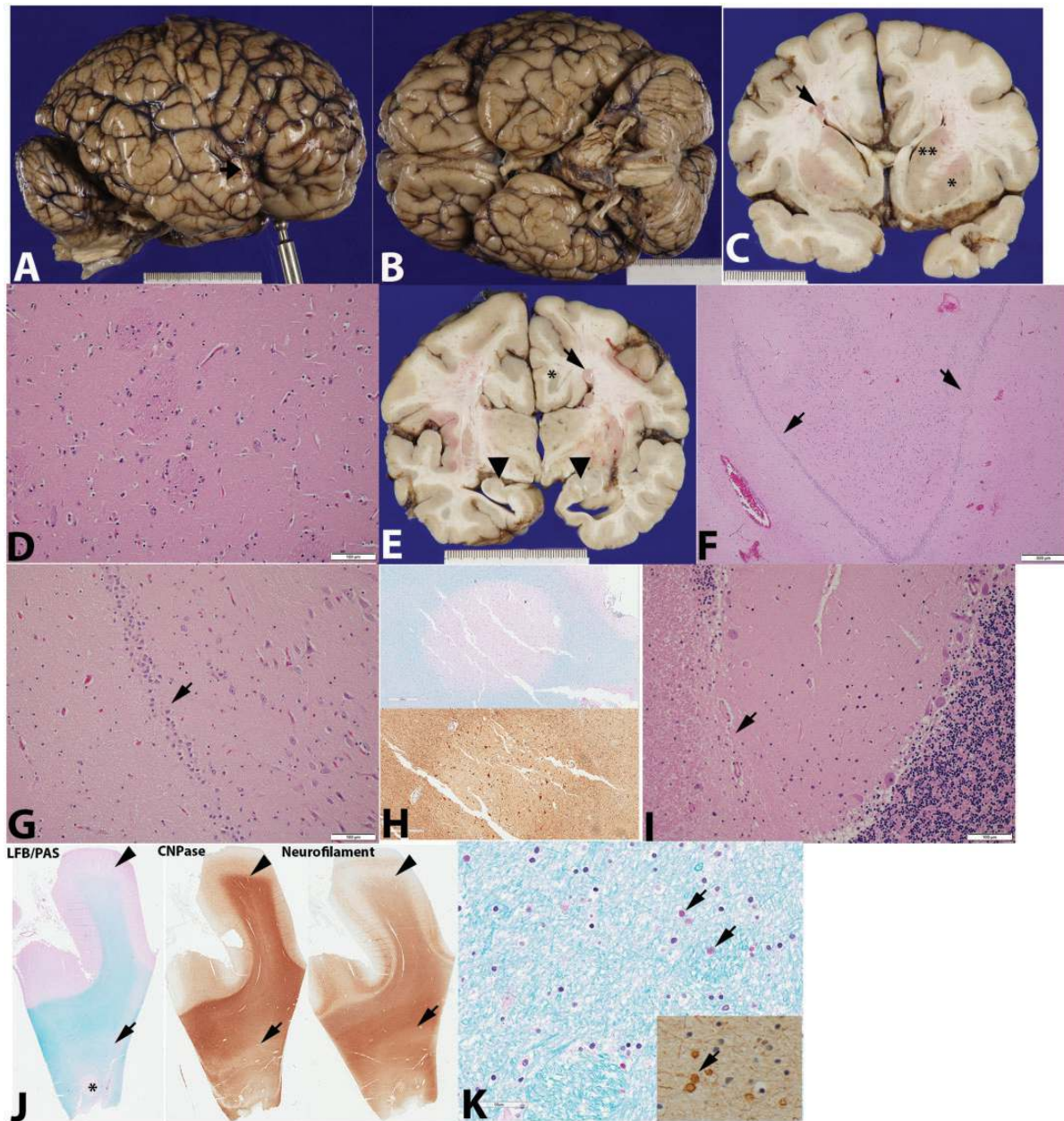


**Figure 1.** A, Lateral view of right cerebral hemisphere showing ill-defined temporal sulcal pattern bilaterally with indistinct superior and inferior temporal sulci and exposed insula (arrow). B, Ventral view of the brain showing that the cerebellum was relatively large compared to the cerebrum and a narrowed space between the temporal lobes. C, Coronal sections reveal generously sized putamen (\*) and caudate head (\*\*\*) bilaterally. The putamen (D) and caudate (not shown) were histologically unremarkable (bar: 100  $\mu$ m). E, The hippocampi were small and poorly rotated (arrowheads) while the cingulate gyri had a complex profile (\*); there was agenesis of the corpus callosum with Probst bundles. Heterotopias were evident in the cerebral white matter (arrows; C and E). F, The dentate gyrus appeared thin due to an overall reduction in granule cell number (arrows; bar: 500  $\mu$ m). G, High magnification confirmed reduced numbers of dentate granule cells (arrow, bar: 100  $\mu$ m). H, Heterotopias were scattered in the white matter in LFB/PAS stained (top) and neurofilament immunostained (bottom) sections. I, Cerebellar cortex showed rare foci of Purkinje and granule cell loss (arrow, bar: 100  $\mu$ m). J, The cerebral white matter showed patchy attenuation of LFB staining and neurofilament, but not CNPase immunoreactivity subjacent to cortex (arrowheads), while deeper areas had patchy attenuation of all three (arrows). The asterisk (\*) corresponds to the heterotopia shown in (H). K, There were scattered PAS-positive structures (arrows) in white matter that also immunolabeled with anti-neurofilament antibodies (inset: arrow; bar: 50  $\mu$ m). LFB/PAS, Luxol fast blue-periodic acid-Schiff.

because the MWS phenotype is only observed in homozygous null mice; in contrast, MWS patients have 1 functional *ZEB2* allele, suggesting that the human nervous system is more reliant on *Zeb2* function or more sensitive to *Zeb2* deficiency than the murine nervous system.<sup>4</sup> The effects of genetic background further complicate matters and conspire to prevent the generation of a single mouse model that encompasses all MWS features.<sup>4</sup>

*Zeb2* is highly expressed in the developing hippocampus and it was small with reduced numbers of dentate granule cells, as reported in *Zeb2* knockout mice.<sup>8</sup> *Zeb2* regulates the differentiation of oligodendrocytes, fostering their maturation, while *Zeb2* deficiency arrests their differentiation and leads to impaired myelin production and repair.<sup>9</sup> This is consistent with the patchy areas of attenuated cerebral white matter myelin identified at autopsy. We also found evidence of possible axonal pathology suggesting that *Zeb2* may be important in the maintenance of axons, as described in models.<sup>10</sup>

*Zeb2* is highly expressed in Bergman glia and knocking *Zeb2* out in murine cerebellar radial glia leads to defective Bergman glia specification and cortical dyslamination.<sup>11</sup> Autopsy showed no cerebellar cortical dyslamination and revealed focal Purkinje and granule cell loss that may be nonspecific. *Zeb2* is important in the development of neocortical and striatal interneurons and is required for proper migration of the former into neocortex.<sup>12,13</sup> The neocortex showed the expected hexalaminar arrangement, but we found heterotopias, which is in keeping with altered neuronal migration. *Zeb2* deficiency alters the differentiation program of interneuron progenitors to favor the production of GABAergic striatal interneurons over neocortical interneurons.<sup>12</sup> No perturbations in neocortical or striatal interneurons were evident at autopsy; however, more sensitive methods would be required to reliably detect a difference in these neuronal populations. Furthermore, it seems unlikely that an alteration in the number of interneurons could account for the seemingly large basal ganglia seen in MWS, which appeared histologically unremarkable.

We report the autopsy neuropathology of a 19-year-old male MWS patient. Autopsy neuropathology correlated well with patient neuroimaging studies and data from MWS mouse models, enhancing our understanding of *ZEB2* function in human brain development and demonstrating the reliability of murine MWS models.

#### Declaration of Conflicting Interests

The author(s) declared no potential conflicts of interest with respect to the research, authorship, and/or publication of this article.

#### Funding

The author(s) received no financial support for the research, authorship, and/or publication of this article.

#### References

1. Mowat DR, Croaker GD, Cass DT, et al. Hirschsprung disease, microcephaly, mental retardation and characteristic facial feature: delineation of a new syndrome and identification of a locus at chromosome 2q22-q23. *J Med Genet.* 1998;35:617–623.
2. Wakamatsu N, Yamada Y, Yamada K, et al. Mutations in SIP1, encoding Smad interacting protein-1, cause a form of Hirschsprung disease. *Nat Genet.* 2001;27:369–370.
3. Cacheux V, Dastot-Le Moal F, Kaariainen H, et al. Loss-of-function mutations in SIP1 Smad-interacting protein 1 result in a syndromic Hirschsprung disease. *Hum Mol Genet.* 2001;10:1503–1510.
4. Epifanova E, Babaev A, Newman AG, et al. Role of *Zeb2/Sip1* in neuronal development. *Brain Res.* 2019;1705:24–31.
5. Garavelli L, Ivanovski I, Caraffi SC, et al. Neuroimaging findings in Mowat-Wilson syndrome: a study of 54 patients. *Genet Med.* 2017;19(6):691–700.
6. Spaggiari E, Baumann C, Alison M, et al. Mowat-Wilson syndrome in a fetus with antenatal diagnosis of short corpus callosum: advocacy for standard autopsy. *Eur J Med Genet.* 2013;56:297–300.
7. Ivanovski I, Djuric O, Caraffi SG, et al. Phenotype and genotype of 87 patients with Mowat-Wilson syndrome and recommendations for care. *Genet Med.* 2018;20(9):965–975.
8. Miquelajauregui A, Van de Putte T, Polyakov A, et al. Smad-interacting protein-1 (*Zfhx1b*) acts upstream of Wnt signaling in the mouse hippocampus and controls its formation. *Proc Natl Acad Sci (USA).* 2007;104(31):12919–12924.
9. Weng Q, Chen Y, Wang H, et al. Dual-mode modulation of Smad signaling by Smad-interacting protein Sip1 is required for myelination in the central nervous system. *Neuron.* 2012;73:713–728.
10. Srivatsa S, Parthasarathy S, Molnár Z, et al. Sip1 downstream effector *ninein* controls neocortical axon growth, ipsilateral branching, and microtubule growth and stability. *Neuron.* 2015;85:998–1012.
11. He L, Yu Kun, Lu F, et al. Transcriptional regulator ZEB2 is essential for Bergmann glia development. *J Neurosci.* 2018;38(6):1575–1587.
12. McKinsey GL, Lindtner S, Trzcinski, et al. Dlx1&2-dependent expression of *Zfhx1b* (*Sip1*, *Zeb2*) regulates the fate switch between cortical and striatal neurons. *Neuron.* 2013;77:83–98.
13. van den Berghe V, Stappers E, Vandesande B, et al. Directed migration of cortical interneurons depends on the cell-autonomous action of Sip1. *Neuron.* 2013;77:70–82.